

Chemical, electrical, and thermal properties of strontium doped lanthanum vanadate

Zhe Cheng, Shaowu Zha, Luis Aguilar, Meilin Liu*

School of Materials Science and Engineering, Georgia Institute of Technology, Atlanta, GA 30332, United States

Received 27 January 2005; received in revised form 17 May 2005; accepted 19 May 2005

Abstract

Strontium doped lanthanum vanadates, $\text{La}_{1-x}\text{Sr}_x\text{VO}_3$ (denoted LSV with $x=0, 0.3, 0.5, 0.7$ and 1.0), were synthesized using a solid-state reaction method. The oxidation and reduction behaviors of LSV were studied using thermogravimetric analysis (TGA) and differential scanning calorimetry (DSC). The chemical stability of LSV in a reducing atmosphere containing H_2S up to 10 vol.% at 950°C was investigated and their electrical conductivity at $500\text{--}1000^\circ\text{C}$ in reducing atmospheres measured with a 4-electrode technique. The coefficient of thermal expansion (CTE) was determined by dilatometry. The electrochemical catalytic activity of LSV as anodes in solid oxide fuel cells (SOFCs) was characterized using impedance spectroscopy. It was found that the $\text{La}_{1-x}\text{Sr}_x\text{VO}_3$ materials with x in the range of $0.3\text{--}0.7$ exhibit good resistance to H_2S , high electrical conductivity and acceptable catalytic activity at elevated temperatures in reducing atmosphere. However, the volume change associated with oxidation/reduction cycle may limit their tolerance to re-oxidation when used as anode materials for SOFCs.

© 2005 Elsevier B.V. All rights reserved.

Keywords: SOFC; Sulfur resistant anode; Strontium doped lanthanum vanadate; Chemical stability; Electrical conductivity; Coefficient of thermal expansion

1. Introduction

It is well known that the Ni/YSZ composite anodes of solid oxide fuel cells (SOFCs) have very poor tolerance to H_2S contaminants in the fuel [1–3]. Although the mechanism of H_2S poisoning is yet to be determined [4], it is certain that exposure to fuels containing more than 100 ppm of H_2S causes great loss to the performance of SOFCs with Ni/YSZ anode [1,3]. The removal of H_2S in the fuel incurs additional complexity and cost. Recently, it was reported that a strontium doped lanthanum vanadate with a nominal composition of $\text{La}_{0.7}\text{Sr}_{0.3}\text{VO}_3$ was used as the anode material for SOFC operating on fuels containing high concentration (up to 10 vol.%) of H_2S [5,6]. The cell performances were among the best reported in the literature for SOFCs using H_2S -containing fuels [3,5–10]. In addition, it was found that $\text{La}_{0.7}\text{Sr}_{0.3}\text{VO}_3$ exhibited selective

oxidation of H_2S and its catalytic activity increased with increasing H_2S concentration [5,6].

Earlier investigations on the lanthanum strontium vanadates (LSV for $\text{La}_{1-x}\text{Sr}_x\text{VO}_3$) were focused on the crystal structure and the related electrical and magnetic properties at temperatures below $\sim 500^\circ\text{C}$ [11–16]. LaVO_3 is a semiconductor while SrVO_3 displays a metallic behavior with conductivity as high as 1000 S cm^{-1} [11,12,15–17] at 800°C in reducing atmosphere. Previous researches showed that LSV exhibits a transition from antiferromagnetic insulator to paramagnetic metal with increasing Sr content near $x=0.2$ [13,15]. To the best of our knowledge, however, none of previous studies were directed towards the understanding of the chemical stability of LSV at high temperatures under various atmospheres, especially in sulfur containing fuels. Neither are there any reports on electrical conductivity nor coefficient of thermal expansion (CTE) of LSV at high temperatures ($>500^\circ\text{C}$) over a wide range of Sr contents. In this paper, we report our recent studies of the chemical stability, electrical conductivity, CTE and electrochemical

* Corresponding author. Tel.: +1 404 894 6114.

E-mail address: meilin.liu@mse.gatech.edu (M. Liu).

activity of LSV under conditions relevant to SOFCs powered by H₂S-containing fuels. Advantages and limitations of La_{1-x}Sr_xVO₃ as possible anode materials for SOFCs using H₂S-containing fuels are also discussed.

2. Experimental

2.1. Preparation of samples

La_{1-x}Sr_xVO₃ powders with $x=0, 0.3, 0.5, 0.7$ and 1.0 were prepared using a solid-state reaction method. The precursors were La₂O₃ (Aldrich, 99.9%), SrCO₃ (Aldrich, 99.9%) and V₂O₅ (Aldrich, 99.6%). La₂O₃ and SrCO₃ were calcinated in air for 2 h at 800 and 300 °C, respectively, to remove the adsorbed moisture. The powders were mixed, ground for 1 h and pressed into pellets at 70 MPa. The pellets were calcinated at 1450 °C for 5 h in the 4% H₂/96% Ar gas mixture followed by repeated grinding and calcination until complete reaction and uniform composition were achieved. The phases were identified using powder X-ray diffraction (XRD, PW1800 X-ray diffractometer, Philips Analytical). The radiation source was Cu-K_α lines.

2.2. Oxidation/reduction behaviors

The oxidation/reduction behaviors of the LSV materials were studied using a simultaneous thermal analyzer (STA, STA1500, Rheometric Scientific), which combines thermogravimetric analysis (TGA) with differential scanning calorimetry (DSC). The amount of sample used for experiment in the STA was ~15 mg. The heating rate was 5 °C/min up to 900 °C. The atmospheres used were air and the 4% H₂/96% Ar mixture for the oxidation and reduction experiment, respectively. In addition, oxidation and reduction of LSV were also carried out in a tube furnace at 900–1550 °C in air or a gas mixture containing 4% H₂ and 96% Ar. The weight change of the sample before and after reaction was measured and the reaction products were analyzed by XRD.

2.3. Evaluation of the chemical stability

Pellets of LSV were put in alumina boats placed in a tube furnace under H₂S-containing atmosphere to evaluate the chemical stability. The furnace was heated up to 950 °C and held for 5 days in a fuel mixture with a nominal composition of 10% H₂S/3% H₂O/87% H₂ (by volume). The chemical compatibility of LSV with yttrium stabilized zirconia (YSZ) was examined by heat-treating a pellet containing 50 wt.% La_{0.7}Sr_{0.3}VO_{0.3} and 50 wt.% YSZ (TZ-8Y, Tosoh) at 1300 °C for 2 h in a gas mixture containing 4% H₂ and 96% Ar.

2.4. Measurement of electrical conductivity

The electrical conductivity of the La_{1-x}Sr_xVO₃ materials was measured using a four-electrode technique. Pellets of

LSV were sintered at 1450–1575 °C for 5 h in a gas mixture containing 4% H₂ and 96% Ar. Rectangular bars with approximate dimensions of 15 mm × 1.5 mm × 1.5 mm were cut from the sintered pellets using a precision diamond saw (Isocut® 4000, Buehler). Four pieces of Pt wires (0.1 mm diameter, annealed at 800 °C in air) were wrapped around the bar; the distance between the two inner electrodes was ~8 mm and the distance between the two outer electrodes was ~14 mm. The bar with the wires was mounted on a piece of alumina substrate by cement (Autostic™ FC6, Flexbar). Pt paste was applied to the contact regions between the bar and the Pt electrodes. The mounted sample was fired at 1050 °C for 2 h in a gas mixture containing 4% H₂ and 96% Ar to obtain a firm bonding and good electrical contact between the Pt wires and the sample. The conductivity was measured at 500–1000 °C in gas mixtures of 3% H₂O/97% H₂ and/or 10% H₂S/3% H₂O/87% H₂. A potentiostat/galvanostat (273A, Princeton Applied Research) was used to draw a constant DC current (I_i) between the two outer electrodes and a multimeter (MY-65, Mastech) to measure the voltage drop between the two inner electrodes (ΔV_i). Typically, five points of ($\Delta V_i, I_i$) were collected at each temperature. Linear mean square regression analysis was performed from the data ($\Delta V_i, I_i$) to obtain the resistance. The bulk conductivity σ was calculated using the following equation [18]:

$$\sigma = \frac{\sigma_m(2 + \varepsilon)}{2(1 - \varepsilon)} \quad (1)$$

in which σ_m is the measured conductivity and ε is the sample porosity. The values for the porosity of the used La_{1-x}Sr_xVO₃ samples are $\varepsilon=0.33$ for $x=0$, $\varepsilon=0.12$ for $x=0.3$, $\varepsilon=0.36$ for $x=0.5$, $\varepsilon=0.22$ for $x=0.7$ and $\varepsilon=0.23$ for $x=1.0$.

2.5. Measurement of the coefficient of thermal expansion (CTE)

The coefficient of thermal expansion for La_{0.7}Sr_{0.3}VO₃ in a reducing atmosphere was measured by a homemade non-contact dilatometer. The sample used for the CTE measurement was sintered at 1550 °C for 5 h in a gas mixture containing 4% H₂ and 96% Ar to achieve a relative density of 97%.

2.6. Characterization of the electrochemical activity

The electrochemical activity of La_{1-x}Sr_xVO₃ with $x=0.3$ and 1.0 was characterized using two-electrode impedance spectroscopy for cells with LSV anode and La_{0.85}Sr_{0.15}MnO₃ (LSM) cathode. The electrolyte was 250 μm thick YSZ and the active electrode area was ~0.25 cm². Paste of LSM cathode was brush painted on the YSZ substrate followed by firing at 1100 °C in air for 2 h. The anode paste was painted onto the other side of the YSZ substrate and fired in-situ at 1000 °C for 2 h before testing. The impedance spectra were measured under open circuit conditions using a

potentiostat/galvanostat (273A, Princeton Applied Research) and a 5210 lock-in amplifier (Princeton Applied Research) interfaced with a computer.

3. Results and discussion

3.1. Structure of LSV materials

Fig. 1 shows the XRD patterns of $\text{La}_{1-x}\text{Sr}_x\text{VO}_3$ with $x=0, 0.3, 0.5, 0.7$ and 1.0 . LaVO_3 ($x=0$) has a tetragonal (distorted perovskite) structure (JCPDS card No. 11-0024) while SrVO_3 ($x=1.0$) has a cubic perovskite structure (JCPDS card No. 42-0039). For the other compositions investigated (i.e., $x=0.3, 0.5$ and 0.7), the XRD patterns match that of a cubic perovskite structure (see JCPDS card No. 33-1343), but the diffraction peaks for those samples are very broad. One explanation of the broadened diffraction peaks is that the A-sites in the ABO_3 perovskite structure are randomly occupied by the Sr and La atoms in these materials. As a result, there may be a broad distribution of the lattice constants throughout the reaction product, resulting in significant broadening of the diffraction peaks in the XRD patterns.

3.2. Redox behavior of LSV materials

Shown in Fig. 2 are the TGA curves for the oxidation of LSV in air with a heating rate of $5^\circ\text{C}/\text{min}$. The oxidation behavior for $\text{La}_{1-x}\text{Sr}_x\text{VO}_3$ with $x=0, 0.3, 0.5$ and 0.7 is very similar. Significant oxidation of these materials started at $\sim 400^\circ\text{C}$ and completed at $\sim 600^\circ\text{C}$. There was only a single stage of weight gain at around 500°C , suggesting that there might be only one type of reactions going on during the entire oxidation processes of these materials. In contrast, the TGA curve for the oxidation of SrVO_3 shows several stages of weight gain. The multiple-step oxidation of SrVO_3 is illustrated more clearly in Fig. 3, which combines both the TGA and the DSC curves.

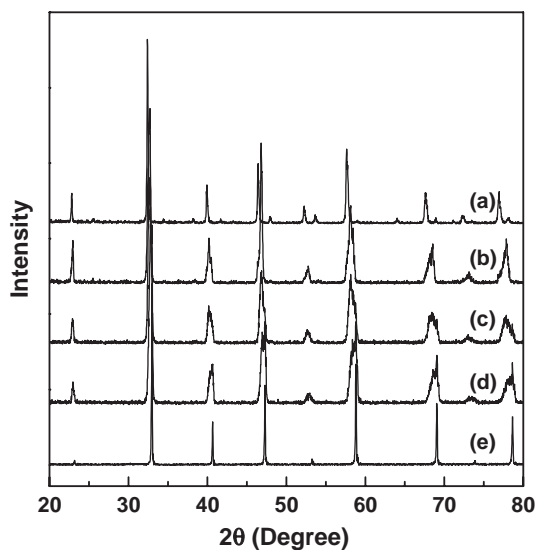


Fig. 1. XRD patterns for the as-synthesized $\text{La}_{1-x}\text{Sr}_x\text{VO}_3$ materials: (a) LaVO_3 , (b) $\text{La}_{0.7}\text{Sr}_{0.3}\text{VO}_3$, (c) $\text{La}_{0.5}\text{Sr}_{0.5}\text{VO}_3$, (d) $\text{La}_{0.3}\text{Sr}_{0.7}\text{VO}_3$ and (e) SrVO_3 .

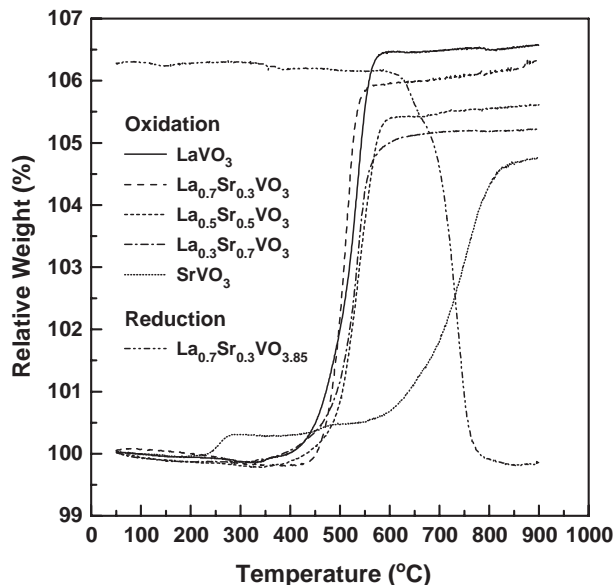


Fig. 2. TGA curves for the oxidation of $\text{La}_{1-x}\text{Sr}_x\text{VO}_3$ with $x=0, 0.3, 0.5, 0.7$ and 1.0 and the reduction of $\text{La}_{0.7}\text{Sr}_{0.3}\text{VO}_{3.85}$. Note that, for the reduction of $\text{La}_{0.7}\text{Sr}_{0.3}\text{VO}_{3.85}$, the weight of the reduction product, presumably $\text{La}_{0.7}\text{Sr}_{0.3}\text{VO}_3$, is taken as unit.

There are three exothermic peaks corresponding to three steps of weight gain. The first step was at around $220\text{--}280^\circ\text{C}$ with a weight gain of $\sim 0.3\%$. The second step was in the $450\text{--}500^\circ\text{C}$ range with a weight gain even smaller ($<0.1\%$). The third step of weight gain was gradual and occurred over a wide range of temperatures from ~ 600 to $\sim 900^\circ\text{C}$. The oxidation temperature of $\text{La}_{1-x}\text{Sr}_x\text{VO}_3$ material is comparable to that of fine nickel powders, which was reported to be oxidized in air at temperature as low as $\sim 400^\circ\text{C}$ [19]. The oxidation of the $\text{La}_{1-x}\text{Sr}_x\text{VO}_3$ ($0 \leq x \leq 1$) materials is expected because the vanadium ions in them are believed to have a mixed valence of $+3$ and $+4$ [11,17]. Upon heat treatment in air, the valence of vanadium increased from $+3$ and/or $+4$ to $+5$. However, it is interesting to observe from the TGA curves that the oxidation

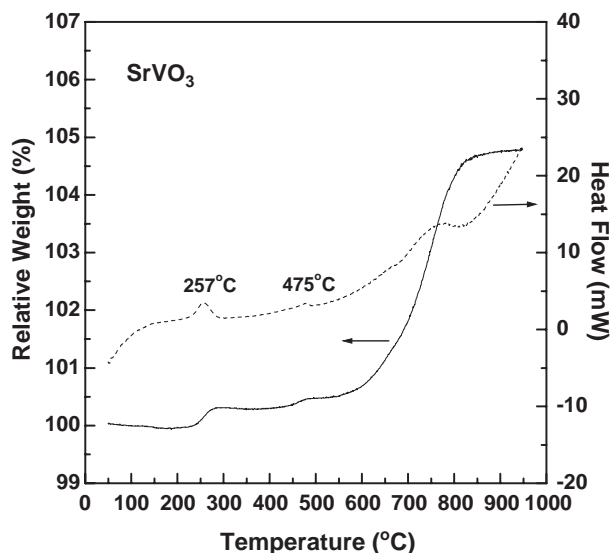


Fig. 3. TGA and DSC curves for the oxidation of SrVO_3 in air.

of SrVO_3 showed multiple steps while the oxidation of other LSV materials appeared to be a single-step process. Since it was reported that SrVO_3 could be non-stoichiometric [12,16,17,20], it is possible that the first step of weight gain during the oxidation of SrVO_3 was related to the combination of oxygen with oxygen vacancy in the SrVO_3 material, i.e., the transformation from $\text{SrVO}_{3-\delta}$ to SrVO_3 . As stated, the weight gain in the first step ($\sim 220\text{--}280\text{ }^\circ\text{C}$) for the oxidation of SrVO_3 was 0.3%; this corresponds to a δ value of 0.03 (i.e., the material before oxidation was $\text{SrVO}_{2.97}$). Such explanation is consistent with the observation of a plateau in the sample weight when $\text{SrVO}_{3-\delta}$ was exposed to the 0.1% O_2/He mixture at $350\text{ }^\circ\text{C}$ [20]. The second step for the oxidation of SrVO_3 may be related to the oxidation of V^{3+} to V^{5+} because the temperature for the second step ($\sim 450\text{--}500\text{ }^\circ\text{C}$) was close to that at which all other materials in the LSV family (containing much more V^{3+}) were oxidized. For SrVO_3 , this step ceased very quickly because the amount of V^{3+} ions in SrVO_3 should be extremely limited. Further weight gain in air at elevated temperature (i.e., the third step) is expected to correspond to the transformation from V^{4+} to V^{5+} , leading to the complete disruption of the original perovskite structure. In comparison to SrVO_3 , there are significant concentrations of V^{3+} ions in other $\text{La}_{1-x}\text{Sr}_x\text{VO}_3$ materials ($x=0, 0.3, 0.5$ and 0.7) [11]. When V^{3+} started to oxidize to V^{5+} at $\sim 500\text{ }^\circ\text{C}$, the resulted structural change may be so large that the structure collapsed and the entire oxidation process (including the oxidation of V^{4+} to V^{5+}) happened within a short period of time. As a result, the oxidation appeared to be a single step process. Nonstoichiometry may also exist in these materials (i.e., $0 \leq x(\text{Sr}) \leq 0.7$); however, the effect during the oxidation process may be less obvious compared with SrVO_3 .

Accompanied by the weight change, the structure of $\text{La}_{1-x}\text{Sr}_x\text{VO}_3$ materials changed dramatically during the oxidation. Fig. 4 shows the XRD patterns of the oxidation products of $\text{La}_{1-x}\text{Sr}_x\text{VO}_3$ with $x=0, 0.3$ and 1.0 . For LaVO_3 and $\text{La}_{0.7}\text{Sr}_{0.3}\text{VO}_3$, the XRD patterns of the oxidation products match that of the monoclinic LaVO_4 (JCPDS card No. 25-0427). The change from the original (distorted) perovskite structure to the monoclinic structure results in a significant change in the unit cell volume. As an example, the oxidation of LaVO_3 is accompanied by a 40% increase in the unit cell volume (calculated from the lattice parameters given in the JCPDS cards). The volume change during the oxidation of $\text{La}_{1-x}\text{Sr}_x\text{VO}_3$ with $x=0$ and 0.3 was verified by the observation that sintered blocks of those materials became loose powders after complete oxidation. The structural change during the oxidation of SrVO_3 is different from that observed for LaVO_3 and $\text{La}_{0.7}\text{Sr}_{0.3}\text{VO}_3$. The XRD pattern of the oxidation product (Fig. 4(c)) matches that of $\text{Sr}_2\text{V}_2\text{O}_7$ (JCPDS card No. 32-1268) with a tetragonal structural. (There is some disagreement about the exact structure of $\text{Sr}_2\text{V}_2\text{O}_7$: both Fotiev and Makarov [21] and Solacolu et al. [22] suggested that it is monoclinic). Interestingly, the volume expansion from SrVO_3 to $1/2\text{ Sr}_2\text{V}_2\text{O}_7$ is also $\sim 40\%$ if the tetragonal structure is assumed. It should be noted that $\text{Sr}_2\text{V}_2\text{O}_7$ is stable in air only up to $\sim 1010\text{--}1120\text{ }^\circ\text{C}$: it decomposes into $\text{Sr}_3\text{V}_2\text{O}_8$ and V_2O_5 in that temperature range [21,22]. Therefore, heat treatment of SrVO_3 at higher temperature ($> \sim 1010\text{ }^\circ\text{C}$) in air may cause the majority of the final oxidation product to be $\text{Sr}_3\text{V}_2\text{O}_8$ since liquid V_2O_5 could be lost significantly. The oxidation of $\text{La}_{0.5}\text{Sr}_{0.5}\text{VO}_3$ and $\text{La}_{0.3}\text{Sr}_{0.7}\text{VO}_3$ at around $900\text{ }^\circ\text{C}$ does not form single-phase products: their XRD patterns indicate

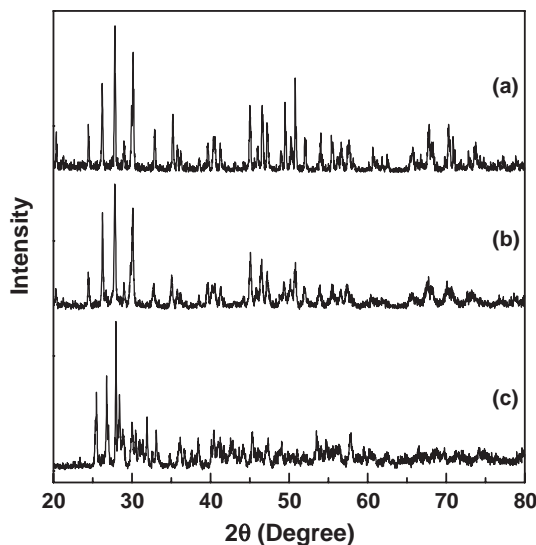
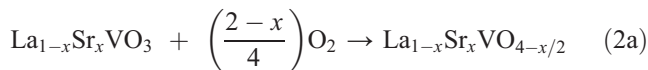


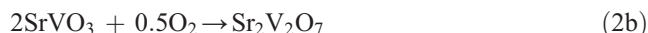
Fig. 4. XRD patterns for (a) LaVO_4 , (b) $\text{La}_{0.7}\text{Sr}_{0.3}\text{VO}_{3.85}$ and (c) $\text{Sr}_2\text{V}_2\text{O}_7$, which are oxidation products of LaVO_3 , $\text{La}_{0.7}\text{Sr}_{0.3}\text{VO}_3$ and SrVO_3 , respectively.

that they are a mixture of $\text{Sr}_2\text{V}_2\text{O}_7$ and $\text{La}_{1-x}\text{Sr}_x\text{VO}_{4-x/2}$ type phase.

The oxidation of stoichiometric $\text{La}_{1-x}\text{Sr}_x\text{VO}_3$ at around $900\text{ }^\circ\text{C}$ could be represented by:



for $x=0$ and 0.3 , or



for $x=1.0$. The number of oxygen in the oxidation product in Eq. (2a) is $4-x/2$ instead of 4 because the charge balance requires the total number of oxygen to be $[3(1-x)+2x+5]/2=4-x/2$ when vanadium is in its fully oxidized state (V^{5+}). Table 1 compares the oxidation yields (by weight) calculated from Eqs. (2a) and (2b) and the yields measured in the experiments. Reasonable agreements are found between calculated and observed values for $\text{La}_{1-x}\text{Sr}_x\text{VO}_3$ with $x=0$ and 0.3 . The largest difference is seen for SrVO_3 . As it is pointed out before, the starting material might have a composition of $\text{SrVO}_{2.97}$ instead of SrVO_3 . The weight change from $\text{SrVO}_{2.97}$ to SrVO_3 (i.e., the first step of oxidation) was 0.3% and the weight change for the entire oxidation process was 4.8%. Hence, the combined yield for the second and third step of the oxidation reaction (presumably from SrVO_3 to $\text{Sr}_2\text{V}_2\text{O}_7$) would be $(1+4.8\%)/(1+0.3\%)=104.5\%$, which matches the value calculated from reaction (2b) when $x=1.0$.

In addition to the oxidation of the LSV materials, the reduction of the oxidation products was also studied. The TGA curve for the reduction of $\text{La}_{0.7}\text{Sr}_{0.3}\text{VO}_{3.85}$ to $\text{La}_{0.7}\text{Sr}_{0.3}\text{VO}_3$ is shown in Fig. 2. The reduction process finished at around $800\text{ }^\circ\text{C}$. Heat treatments also confirmed that the reduction from $\text{La}_{1-x}\text{Sr}_x\text{VO}_{4-x/2}$ to $\text{La}_{1-x}\text{Sr}_x\text{VO}_3$ for $x=0$ and 0.3 could be achieved at around $1000\text{ }^\circ\text{C}$ in 2 h. The reduction of other members in the LSV family (e.g., from $\text{Sr}_2\text{V}_2\text{O}_7$ to SrVO_3) did not seem to complete unless higher temperature or longer time

Table 1

Comparison of the calculated and measured yields for the oxidation reactions of $\text{La}_{1-x}\text{Sr}_x\text{VO}_3$ and the reverse reduction reactions

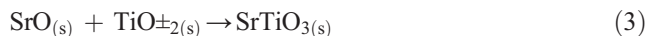
$\text{La}_{1-x}\text{Sr}_x\text{VO}_3$	Oxidation product	Yields of oxidation (%)		Yields of reduction (%)	
		Calculated	Measured	Calculated	Measured
LaVO_3	LaVO_4	106.7	106.5	93.7	93.4
$\text{La}_{0.7}\text{Sr}_{0.3}\text{VO}_3$	$\text{La}_{0.7}\text{Sr}_{0.3}\text{VO}_{3.85}$	106.1	106.0	94.3	93.7
$\text{La}_{0.5}\text{Sr}_{0.5}\text{VO}_3$	$\text{La}_{1-x}\text{Sr}_x\text{VO}_{4-x/2} + \text{Sr}_2\text{V}_2\text{O}_7$	105.7	105.4	94.6	94.1
$\text{La}_{0.3}\text{Sr}_{0.7}\text{VO}_3$	$\text{La}_{1-x}\text{Sr}_x\text{VO}_{4-x/2} + \text{Sr}_2\text{V}_2\text{O}_7$	105.1	105.2	95.1	94.3
SrVO_3	$\text{Sr}_2\text{V}_2\text{O}_7$	104.3	104.8	95.9	NA

was used. Similar phenomena for the reduction of LaVO_4 and $\text{Sr}_2\text{V}_2\text{O}_7$ were reported before [23,24]. The XRD patterns of the reduction products from $\text{La}_{1-x}\text{Sr}_x\text{VO}_{4-x/2}$ and/or $\text{Sr}_2\text{V}_2\text{O}_7$ match those for the original $\text{La}_{1-x}\text{Sr}_x\text{VO}_3$ materials. The measured yield values (by weight) for the reduction reactions are also listed in Table 1 and they agree with the values calculated from the chemical formula. All these data indicate that the oxidation/reduction process is reversible in terms of crystal structure. However, the recrystallization during this process suggests that $\text{La}_{1-x}\text{Sr}_x\text{VO}_3$ may not be used alone as anode support for SOFC because of the large volume change involved in the reactions.

3.3. Chemical stability of LSV materials in H_2S -containing atmosphere

Shown in Fig. 5 are the XRD patterns of the $\text{La}_{1-x}\text{Sr}_x\text{VO}_3$ materials ($x=0, 0.3, 0.5, 0.7$ and 1.0) after exposure to a 10% $\text{H}_2\text{S}/3\% \text{H}_2\text{O}/87\% \text{H}_2$ mixture at 950°C for 5 days. There were almost no changes in the XRD pattern for $\text{La}_{1-x}\text{Sr}_x\text{VO}_3$ materials with $x=0.3, 0.5$ and 0.7 . For LaVO_3 , a partial transformation from the tetragonal distorted perovskite structure (JCPDS card No. 11-0024) to an orthorhombic distorted perovskite structure (JCPDS card No. 36-0141) was observed. For SrVO_3 , the majority of the material transformed into SrS (JCPDS card No. 08-0489).

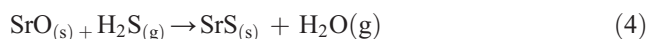
It is interesting to note that the stability of $\text{La}_{1-x}\text{Sr}_x\text{VO}_3$ materials in H_2S -containing atmosphere varies greatly with the Sr content. Since the thermochemical data for complex oxides like $\text{La}_{1-x}\text{Sr}_x\text{VO}_3$ are not available, direct analysis of the stability of those materials is not possible. However, because ABO_3 perovskites could be viewed, in some sense, as an ordered solid solution of the simple oxides of the A-site and B-site cations, the stability of these simple oxides may help to understand the stability of the perovskites. It is known that the Gibbs free energy change from the A-site and B-site simple oxides (e.g., AO and BO_2) to the complex oxides (e.g., ABO_3) would usually be negative [25,26]. For example, the reaction between SrO and TiO_2 to form SrTiO_3 :



is accompanied by a Gibbs free energy change of -138 kJ/mol (see Table 2) at 950°C [25,26]. If the combined free energy change from SrO and TiO_2 to some other phase(s) is more negative than that for the reaction (3) (-138 kJ/mol), thermodynamics predicts that the transformation from SrTiO_3 to these other phase(s) will be energetically favorable.

Similarly, for the $\text{La}_{1-x}\text{Sr}_x\text{VO}_3$ compounds, LaVO_3 can be viewed as $(1/2 \text{La}_2\text{O}_3 + 1/2 \text{V}_2\text{O}_3)$ while SrVO_3 can be viewed as

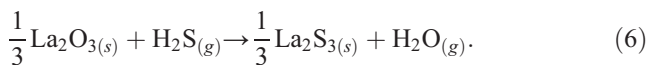
$(\text{SrO} + 1/2 \text{V}_2\text{O}_4)$. Table 2 lists the standard Gibbs formation energy values for some oxides (per mole of O_2), sulfides (per mole of S_2) and gases (per mole of H_2) discussed in this paper [25,26]. For simple oxides of the A-site ions, the reaction between SrO and H_2S is:



and the change in Gibbs free energy at 950°C is given by:

$$\Delta G = -92469 + 8.314 \cdot 1223 \cdot \ln \frac{P_{\text{H}_2\text{O}}}{P_{\text{H}_2\text{S}}} \text{ J/mol} \quad (5)$$

The reaction between La_2O_3 and H_2S is given by:



The change in free energy at 950°C for the reaction (6) is given by:

$$\Delta G = -24561 + 8.314 \cdot 1223 \cdot \ln \frac{P_{\text{H}_2\text{O}}}{P_{\text{H}_2\text{S}}} \text{ J/mol}. \quad (7)$$

The relative partial pressures of H_2S and H_2O under the stability test conditions were 0.1 and 0.03, respectively. Therefore, the change in Gibbs free energy at 950°C for reactions (4) and (6)

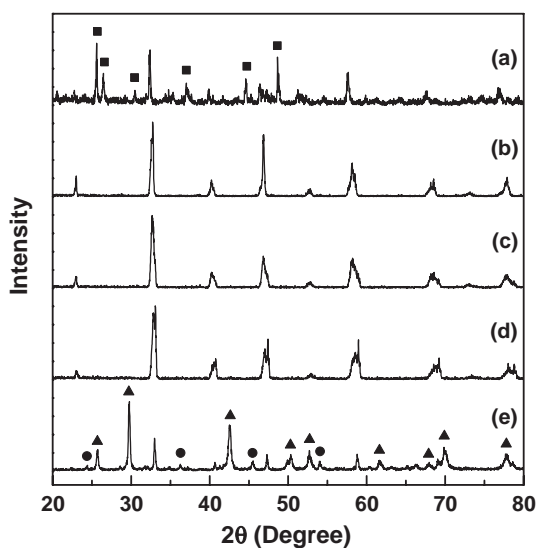


Fig. 5. XRD patterns for the LSV materials after exposure to 10% H_2S at 950°C for 5 days: (a) LaVO_3 , (b) $\text{La}_{0.7}\text{Sr}_{0.3}\text{VO}_3$, (c) $\text{La}_{0.5}\text{Sr}_{0.5}\text{VO}_3$, (d) $\text{La}_{0.3}\text{Sr}_{0.7}\text{VO}_3$ and (e) SrVO_3 . The symbols in the plot represent the impurity phases formed after the exposure: ■ orthorhombic distorted LaVO_3 , ▲ SrS , ● V_2O_3 .

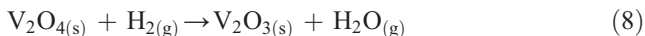
Table 2

Standard Gibbs formation energies, ΔG_f° , for some oxides, sulfides (both in crystal state) and gases (in ideal gas state) at 950 °C (1223K) [25,26]

Material	ΔG_f° at 1223 K (kJ/mol)	Material	ΔG_f° at 1223 K (kJ/mol)
2/3 La ₂ O ₃ (crystal)	−963.984	H ₂ (ideal gas)	0.000
2SrO (crystal)	−938.636	H ₂ S (ideal gas)	−29.991
2/3 SrTiO ₃ (crystal)	−886.682	H ₂ O (ideal gas)	−180.125
TiO ₂ (crystal)	−723.126	2/3 La ₂ S ₃ (crystal)	−712.836
2/3 V ₂ O ₃ (crystal)	−605.723	2SrS (crystal)	−823.303
1/2 V ₂ O ₄ (crystal)	−511.936		

(The standard Gibbs formation energy values were obtained by linear interpolation of the data at 1200 and 1300 K.).

is −105 and −37 kJ/mol, respectively, meaning that the sulfidation of both SrO and La₂O₃ are energetically favorable. For simple oxides of the B-site ions, i.e., V₂O₄ in SrVO₃ and V₂O₃ in LaVO₃, thermodynamics predicts that V₂O₃ is more stable than V₂O₄ in highly reducing atmosphere at elevated temperatures [17]. In fact, the Gibbs free energy change for the reaction:



at 950 °C is:

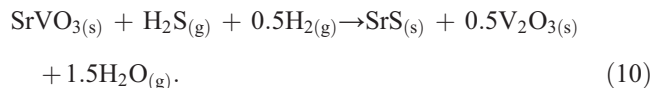
$$\Delta G = -64838 + 8.314 \cdot 1223 \cdot \ln \frac{P_{\text{H}_2\text{O}}}{P_{\text{H}_2}} \text{ J/mol.} \quad (9)$$

Under the condition for the stability test (10% H₂S/3% H₂O/87% H₂ mixture), the free energy change for the reaction (8) would be −99 kJ/mol.

Therefore, for SrVO₃, the simple oxide of the A-site Sr²⁺ ion, SrO, tends to combine with H₂S and form SrS while the oxide of the B-site V⁴⁺ ion, V₂O₄, tends to be reduced to V₂O₃ in the environment of the stability test. Both processes are energetically favorable and the combined Gibbs free energy change (i.e., −105 + (−99)/2 = −154 kJ/mol) may turn out to be more negative than the free energy change when SrO and 1/2 V₂O₄ react to form SrVO₃. (The exact free energy change is not available in the literature, but it is expected to be close to that for the reaction (3) due to the similarity between SrTiO₃ and SrVO₃.) This makes the transformation from SrVO₃ to a mixture of SrS and V₂O₃ energetically favorable. In comparison, for LaVO₃, only the oxide of the A-site La³⁺ ion (La₂O₃) tends to combine with H₂S, and the free energy change (−37 kJ/mol) may be more positive than the free energy change when 1/3 La₂O₃ and 1/3 V₂O₃ react to form 2/3 LaVO₃. (The exact free energy change is also unavailable in the literature.) This makes the transformation from LaVO₃ to other phases (e.g., La₂S₃) energetically forbidden. For other La_{1-x}Sr_xVO₃ materials containing both Sr²⁺ and La³⁺ at the A-sites and both V³⁺ and V⁴⁺ at the B-sites, it is expected that the La³⁺ (also V³⁺) rich materials would be similar to LaVO₃ and be resistant to H₂S while the Sr²⁺ (also V⁴⁺) rich materials would be like SrVO₃ and react with high concentration of H₂S. However, the exact boundary has not been established.

The above explanations were supported by the presence of diffraction lines corresponding to V₂O₃ ((JCPDS card No. 34-0187)) in the XRD pattern of the SrVO₃ material after exposure to H₂S (Fig. 5(e)). It is also consistent with the weight change of the SrVO₃ sample after exposure to H₂S. If it is assumed that only the transformation of Sr²⁺ to SrS and the reduction of V⁴⁺ to

V³⁺ were happening when SrVO₃ was exposed to H₂S, the reaction could be written as:



The expected yield (defined by the ratio of total weight of products to reactants) for the reaction (10) is 104.3%, agreeing well with the measured value of 104.8%. (It should be pointed out that the presence of some minor unidentified diffraction lines in Fig. 5(e) indicates what was actually happening when SrVO₃ was exposed to H₂S/H₂O/H₂ gas mixture could be more complex than the reaction (10) and there may be other reactions proceeding simultaneously.

3.4. Chemical compatibility of LSV with the YSZ electrolyte

Fig. 6 shows the XRD pattern of the pellet of the La_{0.7}Sr_{0.3}VO₃/YSZ mixture after heat treatment at 1300 °C for 2 h in the 4% H₂/96% Ar mixture. Only La_{0.7}Sr_{0.3}VO₃ and YSZ phases could be identified from the pattern, indicating that the La_{0.7}Sr_{0.3}VO₃ material is chemically compatible with the YSZ at temperatures up to 1300 °C in a reducing atmosphere.

3.5. Electrical conductivity of LSV materials

Shown in Fig. 7 are the electrical conductivities of La_{1-x}Sr_xVO₃ (x=0, 0.3, 0.5, 0.7 and 1.0) materials in the 3% H₂O/97% H₂ mixture at various temperatures. The conductivity of LaVO₃ increased slowly with temperature, which is consistent with the trend observed in previous investigations at much lower temperatures [11,13,15]. For La_{0.7}Sr_{0.3}VO₃, typical metallic behavior was observed; the conductivity at 800 °C (149 S cm^{−1}) was more than one order of magnitude higher than that for LaVO₃ (5.7 S cm^{−1}) and was consistent with the literature [17]. As stated earlier, La_{1-x}Sr_xVO₃ is believed to undergo an insulator–metal (I–M) transformation with increasing Sr content when x is near 0.2 [13,15]. As the Sr content increases further, so does the high temperature electrical conductivity. The measured conductivity of La_{0.3}Sr_{0.7}VO₃ in humidified H₂ at 800 °C was around 800 S cm^{−1}. It is not very clear why the electrical conductivity of La_{0.3}Sr_{0.7}VO₃ is so close to that of SrVO₃. When the fuel was switched from humidified H₂ to humidified H₂S balanced by H₂, no significant difference in electrical conductivity was observed for La_{1-x}Sr_xVO₃ with x=0, 0.3, 0.5 and 0.7. This is expected because these materials are chemically stable in the presence of H₂S.

3.6. Coefficient of thermal expansion

Fig. 8 shows the linear expansion of a La_{0.7}Sr_{0.3}VO₃ sample in the temperature range of 200–1000 °C in reducing atmosphere. There was a region in the 450–550 °C range where the thermal expansion shows a sharp bend, indicating a phase transformation in this temperature range. The coefficients of thermal expansion are 9.6 × 10^{−6} and 11.5 × 10^{−6}/K in the temperature ranges of 200–450 °C and 550–950 °C, respectively, which are close to that of YSZ electrolyte [4].

3.7. Electrochemical activity

Previous studies [5,6] suggested that La_{0.7}Sr_{0.3}VO₃ has potential as sulfur-tolerant anode material for SOFCs. In this

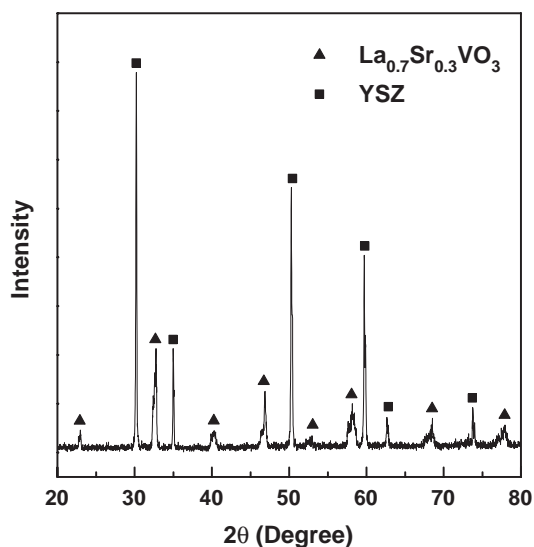


Fig. 6. XRD pattern of the pellet containing 50 wt.% $\text{La}_{0.7}\text{Sr}_{0.3}\text{VO}_3$ and 50 wt.% YSZ after heat treatment at 1300 °C for 2 h in a 4% H_2 /96% Ar gas mixture.

study, the electrochemical activities of LSV with Sr content of 0.3 and 1.0 were studied using impedance spectroscopy in H_2 with or without H_2S . Shown in Fig. 9 are impedance spectra (after subtraction of the bulk resistance) of the button fuel cells with $\text{La}_{0.7}\text{Sr}_{0.3}\text{VO}_3$ or SrVO_3 anodes at 1000 °C. For $\text{La}_{0.7}\text{Sr}_{0.3}\text{VO}_3$, the total interfacial resistances (anode plus cathode) were 2.3 and 1.0 $\Omega\text{ cm}^2$ in the 3% $\text{H}_2\text{O}/97\% \text{H}_2$ and 10% $\text{H}_2\text{S}/3\% \text{H}_2\text{O}/87\% \text{H}_2$ mixtures, respectively. This is consistent with previous investigations [5,6] and demonstrates the good activity of $\text{La}_{0.7}\text{Sr}_{0.3}\text{VO}_3$ towards H_2S oxidation. The SrVO_3 anode also shows decent activity towards H_2 : the total

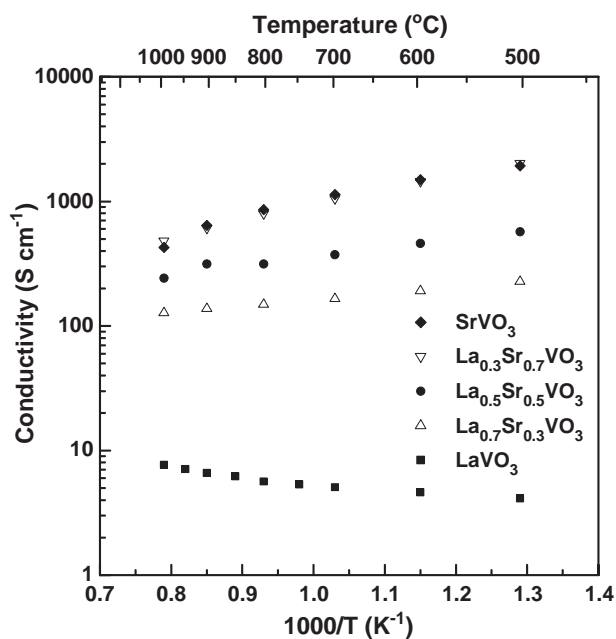


Fig. 7. Electrical conductivities of $\text{La}_{1-x}\text{Sr}_x\text{VO}_3$ with $x=0, 0.3, 0.5, 0.7$ and 1.0 in the 3% $\text{H}_2\text{O}/97\% \text{H}_2$ gas mixture at elevated temperatures.

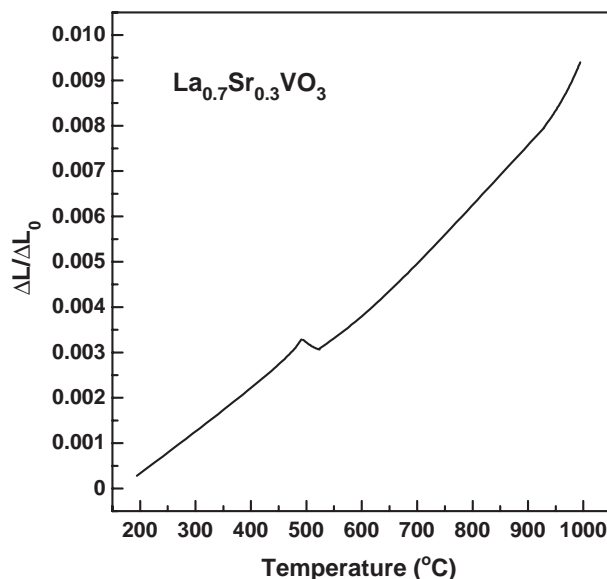


Fig. 8. Linear thermal expansion of $\text{La}_{0.7}\text{Sr}_{0.3}\text{VO}_3$ at temperatures in the 200–1000 °C range in reducing atmosphere. The ramp rate was 2 °C/min.

interfacial resistance was as low as 1.2 $\Omega\text{ cm}^2$ in the 3% $\text{H}_2\text{O}/97\% \text{H}_2$ gas mixture.

4. Conclusions

Some of the chemical and physical properties of $\text{La}_{1-x}\text{Sr}_x\text{VO}_3$ ($x=0, 0.3, 0.5, 0.7$ and 1.0) were investigated. The oxidation/reduction of the $\text{La}_{1-x}\text{Sr}_x\text{VO}_3$ materials involve recrystallization processes. When $\text{La}_{1-x}\text{Sr}_x\text{VO}_3$ were exposed to high concentration of H_2S at elevated temperatures, SrVO_3 reacted readily with H_2S while other compositions (i.e., $x=0, 0.3, 0.5$ and 0.7) showed resistance to H_2S . For $x=0.3$, the LSV material displayed good chemical and thermal compatibility with YSZ. The electrical conductivity of $\text{La}_{1-x}\text{Sr}_x\text{VO}_3$ in humidified H_2 at 800 °C increased from $\sim 5.7 \text{ S cm}^{-1}$ for $x=0$ to $\sim 800\text{--}900 \text{ S cm}^{-1}$ for $x=0.7\text{--}1.0$. LSV materials show decent activity towards the electrochemical oxidation of H_2 and/or H_2S . The results

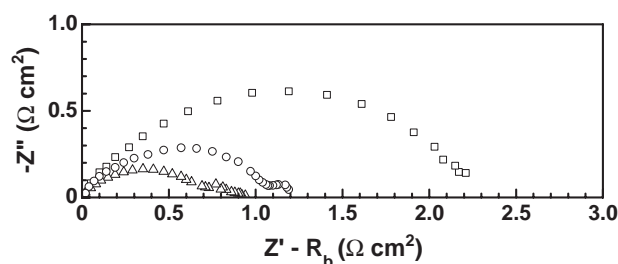


Fig. 9. Impedance spectra for three different cells operating at 1000 °C: □ stands for the cell with $\text{La}_{0.7}\text{Sr}_{0.3}\text{VO}_3$ anode operating in the 3% $\text{H}_2\text{O}/97\% \text{H}_2$ gas mixture; ○ stands for the cell with $\text{La}_{0.7}\text{Sr}_{0.3}\text{VO}_3$ anode operating in the 10% $\text{H}_2\text{S}/3\% \text{H}_2\text{O}/87\% \text{H}_2$ gas mixture; △ stands for the cell with SrVO_3 anode operating in the 3% $\text{H}_2\text{O}/97\% \text{H}_2$ gas mixture.

obtained in this study suggest that $\text{La}_{1-x}\text{Sr}_x\text{VO}_3$ with $0.3 \leq x \leq 0.7$ may be used as anode catalyst for SOFC running on fuels containing high concentration of H_2S . However, the volume change associated with the oxidation/reduction cycle implies that these materials may have limited tolerance to re-oxidation when used as anode materials for SOFC.

Acknowledgements

This work was supported by Shell Global Solutions and DOE-NETL SECA Core Technology Program (under Award Number: DE-FC26-04NT42219). We would like to thank Dr. Jim K. Lee of Georgia Institute of Technology for the measurement of the coefficients of thermal expansion.

References

- [1] D.W. Dees, U. Balachandran, S.E. Dorris, J.J. Heiberger, C.C. McPheeters, J.J. Picciolo, Proceedings of the First International Symposium on Solid Oxide Fuel Cells, The Electrochemical Society Proceedings Series, vol. 89–11, The Electrochemical Society, Pennington, NJ, 1989, p. 317.
- [2] Y. Matsuzaki, I. Yasuda, Solid State Ionics 132 (2000) 261.
- [3] R. Mukundan, E.L. Brosha, F.H. Garzon, Electrochemical and Solid-State Letters 7 (2004) A5.
- [4] N.Q. Minh, T. Takahashi. Science and Technology of Ceramic Fuel Cells, Elsevier Science, Netherlands, 1995, p.87, p. 157 and p. 209.
- [5] L. Aguilar, S. Zha, S. Li, J. Winnick, M. Liu, Electrochemical and Solid-State Letters 7 (2004) A324.
- [6] L. Aguilar, S. Zha, Z. Cheng, J. Winnick, M. Liu, Journal of Power Sources 135 (2004) 17.
- [7] N.U. Pujare, K.W. Semkow, A.F. Sammells, Journal of the Electrochemical Society 134 (1987) 2639.
- [8] D.R. Peterson, J. Winnick, Journal of the Electrochemical Society 145 (1998) 1449.
- [9] C. Yates, J. Winnick, Journal of the Electrochemical Society 146 (1999) 2841.
- [10] M. Liu, G. Wei, J. Luo, A.R. Ranger, K.T. Chuang, Journal of the Electrochemical Society 150 (2003) A1025.
- [11] P. Dougier, A. Casalot, Journal of Solid State Chemistry 2 (1970) 396.
- [12] P. Dougier, J.C.C. Fan, J.B. Goodenough, Journal of Solid State Chemistry 14 (1975) 247.
- [13] P. Dougier, P. Hagemuller, Journal of Solid State Chemistry 15 (1975) 158.
- [14] A. Nozaki, H. Yoshikawa, T. Wada, H. Yamauchi, S. Tanaka, Physical Review B 43 (1991) 181.
- [15] A.V. Mahajan, D.C. Johnston, D.R. Torgeson, F. Borsa, Physical Review B 46 (1992) 10973.
- [16] V. Giannakopoulou, P. Odier, J.M. Bassat, J.P. Loup, Solid State Communications 93 (1995) 579.
- [17] S. Hui, A. Petric, Solid State Ionics 143 (2001) 275.
- [18] H.J. Jurechke, R. Landauer, J.A. Swanson, Journal of Applied Physics 27 (1956) 838.
- [19] M.S. Hegde, D. Larcher, L. DuPont, B. Beaudoin, K. Tekaia-Elhsissen, J.-M. Tarascon, Solid State Ionics 93 (1997) 33.
- [20] M.R. Rey, P.H. Dehaut, J.C. Joubert, B. Lambert-Andron, M. Cyrot, F. Cyrot-Lackmann, Journal of Solid State Chemistry 86 (1990) 101.
- [21] A.A. Fotiev, V.A. Makarov, Soviet Physics. Crystallography 14 (1970) 621.
- [22] S. Solacolu, R. Dinescu, M. Zaharescu, Revue Roumaine de Chimie 17 (1972) 311.
- [23] T. Palanisamy, J. Gopalakarshnan, M.V.C. Sastri, Zeitschrift fur Anorganische und Allgemeine Chemie 415 (1975) 275.
- [24] H.-Zh. Li, L.-M. Liu, K.P. Reis, A.J. Jacobson, Journal of Alloys and Compounds 203 (1994) 181.
- [25] M.W. Chase Jr., C.A. Davies, J.R. Downey Jr., D.J. Frurip, R.A. McDonald, A.N. Syverud, JANAF Thermochemical Tables, Third edition, American Chemical Society, Washington D.C, 1985.
- [26] M. Binnewies, E. Milke, Thermochemical Data of Elements and Compounds, Wiley-VCH, Weinheim, NY, 1999.